

Giant magnetoresistance and long-range antiferromagnetic interlayer exchange coupling in (Ga,Mn)As/GaAs:Be multilayers

Sunjae Chung,¹ Sanghoon Lee,^{1,*} J.-H. Chung,¹ Taehee Yoo,¹ Hakjoon Lee,¹ B. Kirby,² X. Liu,³ and J. K. Furdyna³

¹*Department of Physics, Korea University, Seoul 136-701, Korea*

²*NIST Center for Neutron Research, Gaithersburg, Maryland 20899, USA*

³*Department of Physics, University of Notre Dame, Notre Dame, Indiana 46556, USA*

(Received 7 July 2010; published 13 August 2010)

We report the observation of the giant magnetoresistance effect in semiconductor-based GaMnAs/GaAs:Be multilayers. Clear transitions between low-field-high-resistance and high-field-low-resistance states are observed in selected samples with Be-doped nonmagnetic spacers. These samples also show negative coercive fields in their magnetic hysteresis and antiferromagnetic (AFM) splittings in polarized neutron reflectivity. Our data indicate that the AFM interlayer exchange couplings in this system occur over much longer periods than predicted by current theories, strongly suggesting that the coupling in III-V semiconductor-based magnetic multilayers is significantly longer ranged than in metallic systems.

DOI: [10.1103/PhysRevB.82.054420](https://doi.org/10.1103/PhysRevB.82.054420)

PACS number(s): 72.15.Gd, 75.47.De, 75.50.Pp

I. INTRODUCTION

The observation of giant magnetoresistance (GMR) (Refs. 1 and 2) in magnetic multilayers contributed greatly to the inception of the new field of “spintronics,”³ in which both the charge and the spin degrees of freedom of charge carriers are exploited. This new functionality has been serving as the key ingredient in electrically controlled magnetic memory and sensor devices, as well as high-density read-head technology.⁴ In metallic magnetic multilayers, the GMR effect is achieved when the interlayer exchange coupling (IEC) between adjacent magnetic layers is antiferromagnetic (AFM). In this situation the amount of current flow is greatly enhanced when the relative magnetization alignments in adjacent magnetic layers is changed from antiparallel to parallel by an external field. Since the original discovery in (Fe/Cr)_n multilayers,⁵ the AFM IEC has been observed in a variety of ferromagnetic metallic^{6–9} and semiconductor^{10,11} multilayer systems. Mn-doped GaAs ferromagnetic semiconductor layers are also expected to be suitable for spintronic applications and several types of spintronic devices based on this system have already been fabricated and tested.^{12,13} The potential advantages of GaMnAs lie not only in the well-established semiconductor technology but also in the tunability of the spintronic properties via carrier density control.^{14–16} Owing to this advantage, exchange interaction of GaMnAs with other ferromagnetic metals has been investigated in several types of metal/GaMnAs hybrid structures.^{17–19} In order to realize information storage applications involving this system, it is highly desirable to achieve AFM IEC in GaMnAs-based multilayer structures, that can then lead to the GMR effect.

Significant effort has already been made aimed at the understanding of IEC in GaMnAs-based multilayers, both in theory and in experiments. Theoretical studies of IEC conducted so far on this system are primarily based on interactions of the Ruderman-Kittel-Kasuya-Yosida (RKKY) type, exploiting the Fermi-wavelength-dependent susceptibility of the electron gas. One of the major theoretical predictions is the oscillation of the ferromagnetic (FM) and AFM interlayer

coupling^{20–23} as a function of carrier density and of the nonmagnetic spacer thickness. Experimental observations of GaMnAs-based multilayer structures, however, including trilayers and superlattices (SLs),^{24–29} have mostly shown FM IEC. It was only very recently that direct evidence of AFM IEC was reported in GaMnAs/GaAs:Be multilayers with intentionally doped spacers.³⁰ Specifically, Chung and coauthors observed that spontaneous robust AFM IEC was achieved when *p*-type doping was introduced in the nonmagnetic GaAs spacers. While this experimental work confirmed the importance of carrier density control for the spontaneous AFM IEC, as predicted by theory, the GMR effect in the electrical transport in this system, which is of key importance for spintronic device applications, still remained to be observed. In this paper we report the experimental verification that the AFM IEC in GaMnAs-based multilayers does lead to the GMR effect, and that the FM IEC results in its absence, similar to metallic ferromagnetic multilayers.

II. EXPERIMENTS

Two series of GaMnAs/GaAs SLs, A and B, were prepared using low-temperature molecular-beam epitaxy on GaAs (001) substrates. Each SL consists of ten ferromagnetic Ga_{0.97}Mn_{0.03}As layers [with a thickness $d_M=6.9$ nm ≈ 24 monolayer (ML)] separated by nonmagnetic GaAs layers. The GaAs spacers in series B were doped with Be during the growth while those in series A were not. The hole densities of Ga_{0.97}Mn_{0.03}As and GaAs:Be layers are estimated from Hall measurements on epilayers that were grown using identical growth conditions to be 1.19×10^{20} cm⁻³ and 1.20×10^{20} cm⁻³, respectively. We label the SL samples as A1–A4 and B1–B4 in order of increasing spacer thickness, as summarized in Table I. The two series are distinguished only by the Be doping of the GaAs spacers, except for the small thickness difference between A1 and B1. For transport measurements, the multilayer films were patterned by photolithography and chemical wet etching into 300 $\mu\text{m} \times 1500 \mu\text{m}$ rectangles, with the long dimension (the current direction) parallel to the $[1\bar{1}0]$ magnetic hard

TABLE I. Summary of dimensions of GaMnAs/GaAs multilayers investigated in this work. d_M and d_N denote thicknesses of the magnetic GaMnAs and nonmagnetic GaAs layers, respectively, whereas $d_{SL}(=d_M+d_N)$ is the superlattice period in units of nanometer. The values given in nanometer can be converted to number of monolayers by multiplying with the factor 3.54 ML/nm.

Undoped	d_M (nm)	d_N (nm)	d_{SL} (nm)	Be doped	d_M (nm)	d_N (nm)	d_{SL} (nm)
A1	6.9	0.7	7.6	B1	6.9	1.2	8.1
A2	6.9	2.3	8.2	B2	6.9	2.3	8.2
A3	6.9	3.5	10.4	B3	6.9	3.5	10.4
A4	6.9	7.1	14.0	B4	6.9	7.1	14.0

axis. MR was measured with the external magnetic field applied in the plane of the sample. The angle between the applied field and the $[1\bar{1}0]$ direction is denoted by φ . Magnetization measurements were carried out using a commercial vibrating sample magnetometer with the field applied along the $[110]$ direction. Polarized neutron reflectivity was measured using the NG1 cold neutron-polarized reflectometer at the NIST Center for Neutron Research.

III. RESULTS AND DISCUSSION

Figure 1 shows the summary of the MR data measured at 30 K with the magnetic field applied near the $[110]$ direction. At this temperature the magnetic anisotropy field is known to be reduced below the strength of IEC to a degree sufficient for MR to reveal the presence of spontaneous IEC. The data can be classified into two groups with contrasting behaviors: Group 1 (samples A1–A4, B1, and B2) and Group 2 (samples B3 and B4). Group 1 shows positive MR over a wide range of applied fields with the rate of change larger at low fields. The field-dependent increase in resistance is ascribed to anisotropic MR (AMR), which is determined by the angle between the magnetization vector and the direction of the current. Such positive AMR is typical of ferromagnetic GaMnAs and is normally observed in single-layer films as well.^{31,32} From this we infer that the IEC between the ferromagnetic $\text{Ga}_{0.97}\text{Mn}_{0.03}\text{As}$ layers in Group 1 is most likely FM.

In striking contrast, the samples in Group 2 show negative MR that occurs abruptly within small ranges of magnetic fields. In the case of B3, on increasing the field the resistance is nearly constant below $B \approx 35$ Oe or above $B \approx 80$ Oe, and the transition between the two states occurs through several stepwise decrease in the resistance. A hysteresis is observed on the return path (i.e., on decreasing the field) because the reverse transition occurs at lower fields. Nevertheless, the zero-field resistance is fully recovered at $B \approx 25$ Oe. When the reverse field is applied, the observed MR is exactly symmetric about zero. Such spontaneous recovery of the zero-field resistivity strongly suggests that there is a spontaneous coupling between the magnetic layers. The presence of the AFM IEC in this same sample, along with its field switching behavior, has previously been confirmed using polarized

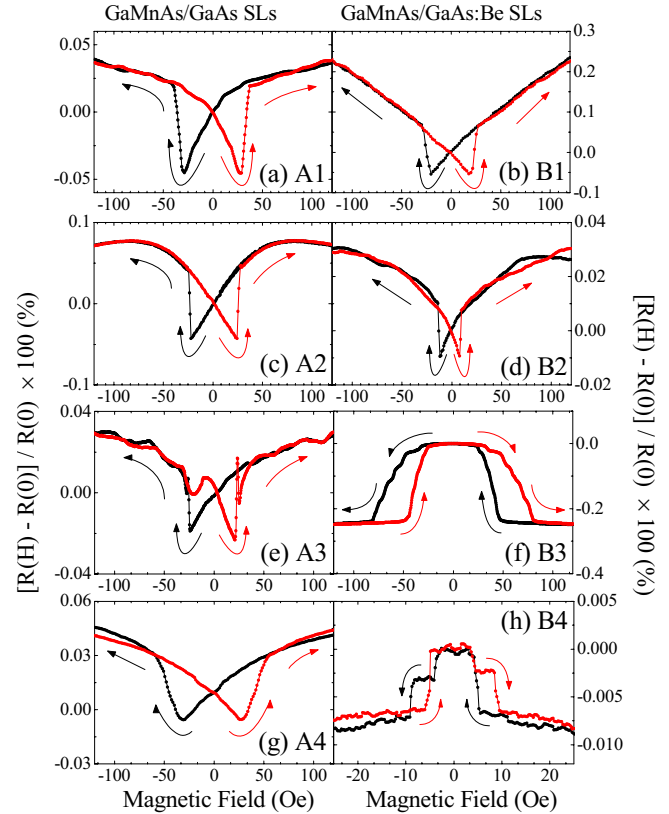


FIG. 1. (Color online) Magnetoresistance of GaMnAs/GaAs multilayers measured with magnetic field applied near the $[110]$ direction at $T=30$ K. Although the AMR typical for GaMnAs layers dominates the MR observed in most of the samples, GMR is clearly seen in samples B3 and B4, indicating the presence of AFM IEC in those specimens. The arrows indicate the direction of field scan.

neutron reflectivity.³⁰ Thus we conclude that the effect observed in the present magnetotransport measurements is the GMR effect often observed in metallic ferromagnetic multilayers exhibiting AFM IEC,^{1,4} that is ascribed to changes in the spin-dependent scattering cross section of charge carriers. This result confirms that it is possible to realize GMR devices using GaMnAs-based ferromagnetic semiconductor structures.

Although the AFM IEC in B3 has already been reported in our previous work,³⁰ the result presented in this work provided another surprise, i.e., based on observing similar AFM IEC also in sample B4. The thickness of the nonmagnetic spacers in B4 is two times greater than in B3 and its SL period is as large as 49.5 ML (14 nm). Figure 1 shows that the magnitude of GMR in B4 is smaller by two orders of magnitude, but the overall MR behavior is essentially identical, featuring similar stepwise transitions, hysteresis, and symmetry. We note that such GMR is absent in other samples in series B (those with shorter period) and in the all samples in series A.

Since the observation of AFM IEC in large-period SLs is unexpected, we provide further evidence to corroborate its existence. Summarized in Fig. 2 are magnetic hystereses of SL samples measured with the field applied along the $[110]$

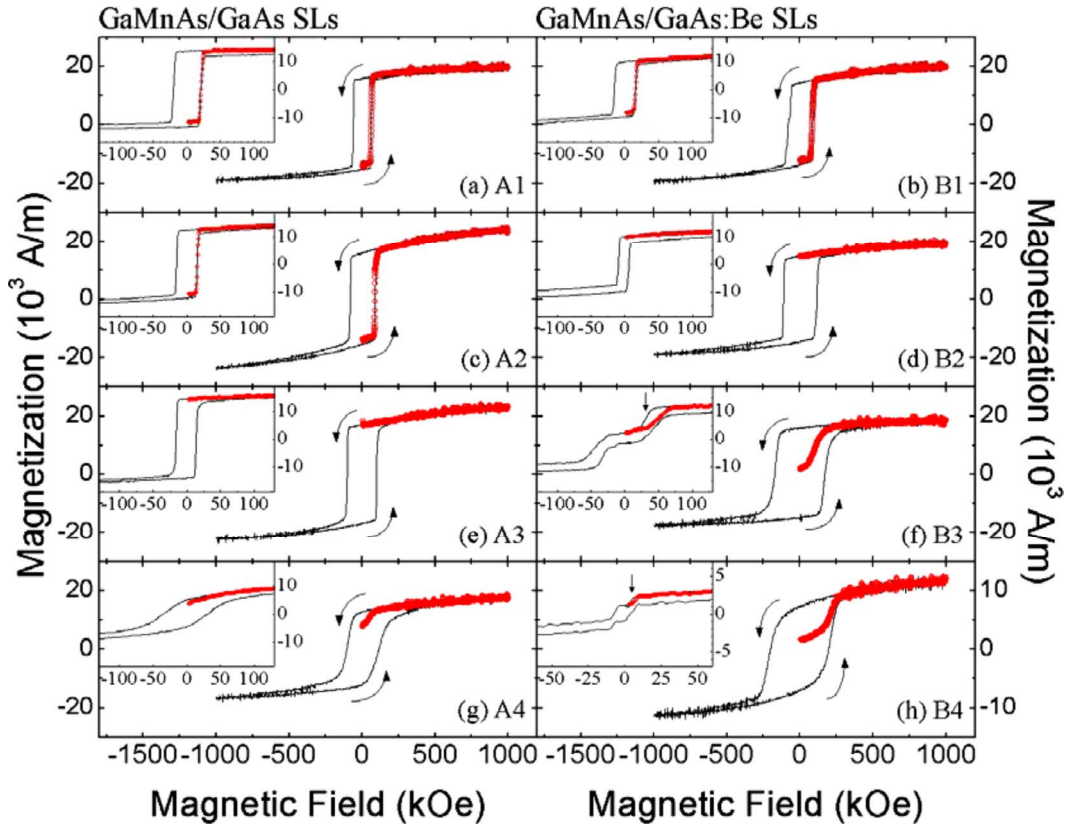


FIG. 2. (Color online) Hysteresis for GaMnAs/GaAs multilayers. The main panels show hysteresis curves obtained at $T=5$ K for the SL samples with undoped spacers (series A: left column) and Be-doped spacers (series B: right column). Red circles indicate the initial magnetization sweeps after zero-field cooling. The arrows indicate the direction of field scan. The insets show the hysteresis curves obtained at $T=30$ K. The arrows in the inset of panels (f) and (h) mark the negative coercive fields.

direction. The measurements were performed after cooling the samples in zero field down to the desired temperatures. At $T=5$ K all samples show square-shaped loops, indicating collective FM-like behavior. Note, however, that the initial magnetization curves of the samples in Group 2, shown as red circles in Fig. 2, differ from the main hysteresis loops obtained after field saturation. Their initial net magnetization starts out at approximately zero and merges with the main hysteresis loop only after the field is increased to near saturation. This behavior is consistent with the presence of the AFM IEC that leads to antiparallel configuration between the ferromagnetic GaMnAs layers. The zero magnetization is, however, not recovered when the field is reduced back to zero on the return trip from saturation because of the strong magnetic anisotropy characteristic of GaMnAs. The magnetization of all the layers is then locked into parallel alignment, all the layers responding together to the external field.³⁰ Similar spin locking due to magnetic anisotropy has been observed in EuS/PbS superlattices³³ and Fe/Nb multilayers³⁴ in neutron-scattering experiments.

Since spin locking can be avoided when the magnetic anisotropy is reduced, we repeated the measurements at $T=30$ K and plotted the results in the insets in Fig. 2. It is easy to see that at this temperature even the main loops look very different in the two groups. Group 1, except for sample A4, shows approximately square-shaped hysteresis loops similar to those observed at 5 K. The IEC in these samples is

therefore most likely ferromagnetic. In contrast, Group 2 shows complicated loops, with additional steps. The presence of a negative coercive field, marked by arrows in the insets in Fig. 2, provides strong evidence for the presence of AFM IEC in Group 2 magnetic multilayers,^{35,36} its magnitude being directly related to the strength of the IEC field. The negative coercive fields, ~ 40 Oe for B3 and ~ 5 Oe for B4, are consistent with the negative coercive fields observed in the MR data [see Figs. 1(f) and 1(g)].

We also measured polarized neutron reflectivity of the B4 sample in order to obtain a quantitative estimate of the magnetization in the AFM-coupled multilayers. The experimental setup of the polarized neutron reflectivity measurements is identical to that described in Ref. 30. As in that earlier work, only the two polarized neutron reflectivity channels with no flip of neutron spins due to the sample are explicitly shown in Fig. 3. These two channels, (++) and (--) respectively, are relatively strong and are ascribed to the magnetization components parallel to the applied field. In comparison, the other two channels, in which neutron spins flip due to the sample, are substantially weaker and are ascribed to the magnetization components perpendicular to the applied field. We find that the polarized neutron reflectivity curves measured on the B4 sample agree well with the expected dimensions of the superlattice and their field dependence is very similar to that measured on B3.³⁰ Figure 3(a) shows that the Bragg peak appears at $Q_{SL}=2\pi/(d_M+d_N)=0.045/\text{\AA}$, corresponding

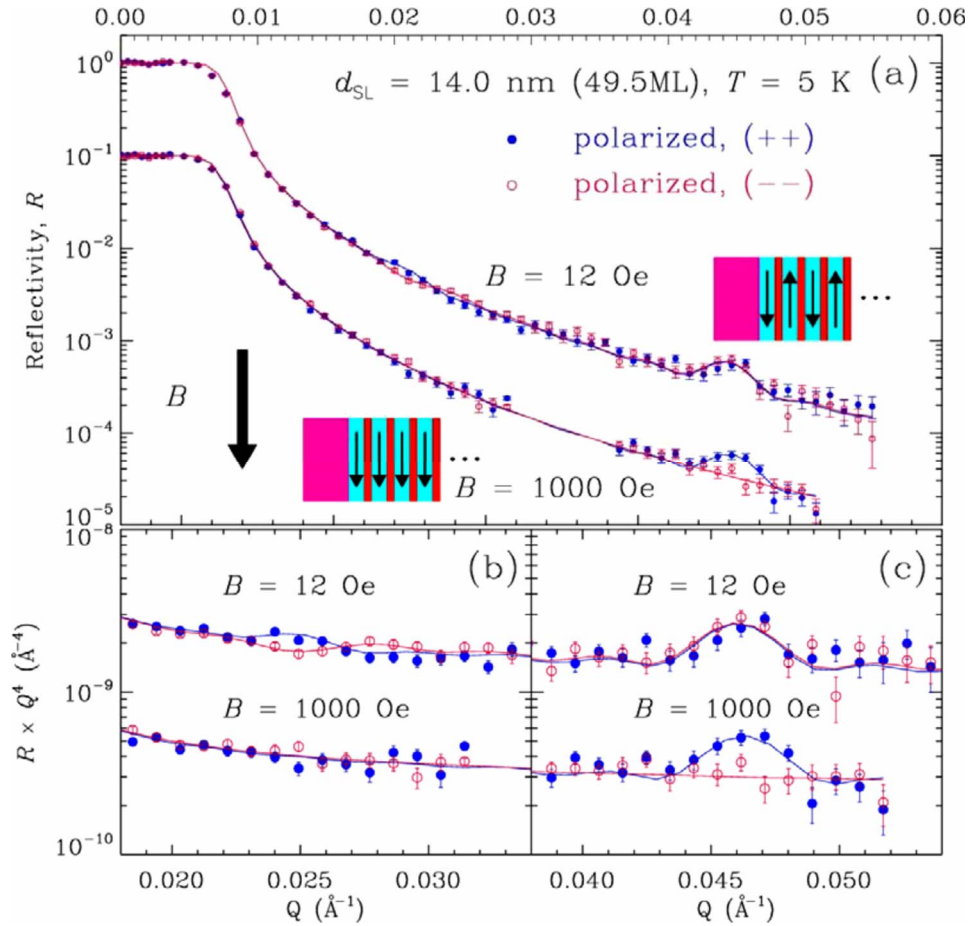


FIG. 3. (Color online) Polarized neutron reflectivity of Be-doped B4 sample with the SL period $d_{SL}=14.0$ nm (49.5 ML). The filled and open circles are the two nonspin-flip reflectivity curves, $(++)$ and $(--)$, respectively, measured at 5 K and corrected for polarization efficiency. The solid lines are calculations using models with either AFM or FM interlayer alignments, as schematically depicted next to the curves. Shown in (b) and (c) are closeup views on the characteristic splittings of the AFM and FM alignments, respectively.

to the structural superlattice period of 14.0 nm. At low field ($B=12$ Oe) it also reveals a splitting between the two curves near the wave vector corresponding to twice the SL period, that is, $Q_{AFM}=Q_{SL}/2=0.023/\text{\AA}$ [see Fig. 3(b)]. At high fields ($B=1000$ Oe), the splitting near Q_{AFM} is suppressed and a different splitting is observed for the Bragg peak [see Fig. 3(c)]. We have fitted the reflectivity data using a simple model that assumes uniform magnetization in all of the magnetic layers. The model calculations, shown as solid lines in Fig. 3, confirm that the interlayer spin alignments are indeed AFM and FM at the low and the high fields, respectively. From the best fit parameters we obtain the net magnetization along the field direction to be $1.2 \pm 0.2 \mu_B$ per Mn ion at $B=12$ Oe. The obtained value is approximately half of the value for B3, which is consistent with the saturation magnetizations shown in Fig. 2. It is also seen that the interface roughness of the SL sample is less than 1.5 nm, which is substantially less than the thickness of either layer. Given the presence of a cooling field of approximately 1 Oe parallel to the magnetic easy axis, the observation of the AFM splitting confirms that spontaneous AFM IEC exists in B4. We note, however, that the AFM IEC of sample B4 is significantly weaker than in sample B3, as indicated both by the GMR results and by magnetization measurements. When the tem-

perature was increased, the magnetization decreased gradually and became too weak at 30 K for the AFM splitting to be observable. Consistently, the magnetization data indicates that the net magnetization is reduced by a factor of 4 when the temperature is raised from 5 to 30 K.

We note that the AFM splitting of the polarized neutron reflectivity is not observed in samples in Group 1. When combined with the results of MR and magnetization measurements, it appears that, to have AFM IEC, it is essential to have extrinsic carrier doping in the nonmagnetic spacers at a level similar to the carrier concentration in the ferromagnetic layers. It is interesting that the robust AFM IEC persists up to very large SL periods, e.g., $d_{SL}=49.5$ ML, which is quite surprising. Figure 4 shows an approximate IEC phase diagram deduced from our experimental results. The average carrier concentrations of the SL samples were estimated using the following relation: $\bar{p}=(d_M p_M+d_N p_N)/(d_M+d_N)$, where $p_M=1.19 \times 10^{20}/\text{cm}^3$, $p_{N,A} \approx 0$, and $p_{N,B}=1.2 \times 10^{20}/\text{cm}^3$. The diagram shows that the boundary between the FM IEC and AFM IEC should occur at much larger distances (e.g., $d_{SL} \approx 34$ ML) than those predicted by theory. Previous theoretical studies based on the RKKY interaction typically expect that the magnitude of IEC will become too weak for multilayer periods beyond

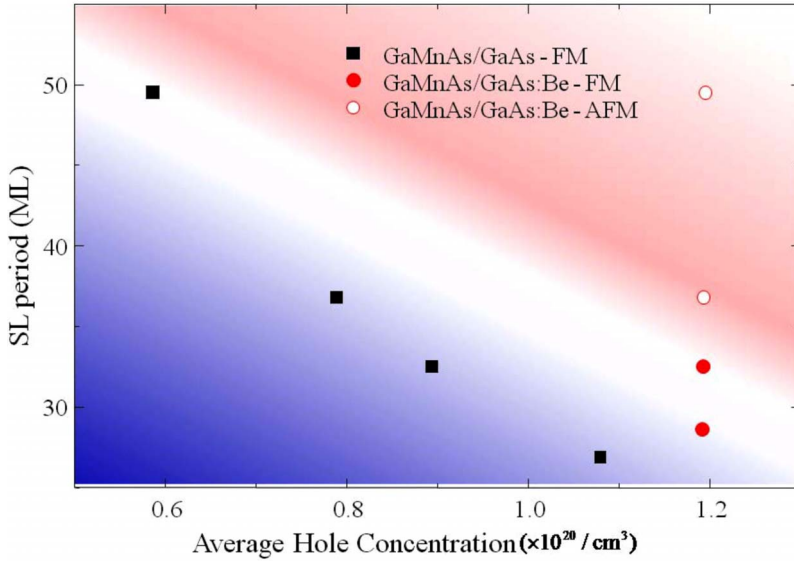


FIG. 4. (Color online) Phase diagram of IEC for GaMnAs/GaAs multilayers as a function of superlattice period and average carrier concentration. The solid and open symbols indicate FM and AFM IEC, respectively. Experimentally observed FM IEC and AFM IEC regions correspond approximately to the blue and red colors, respectively.

10 ML or so, which is in clear contradiction with our experimental results, which demonstrate the existence of strong FM or AFM IEC beyond 30 ML, up to at least 49 ML.

One may suspect dipole interaction (such as that reported for metallic multilayers³⁷), as a possible mechanism for the long-range IEC in GaMnAs/GaAs:Be multilayer structures. However, if dipole interaction plays a major role for long-range AFM IEC, one would expect a systematic increase in AFM IEC as the spacer thickness is decreased. Furthermore, the AFM IEC should also be observed in GaMnAs/GaAs multilayers in which the spacer is not doped by Be since the structural dimensions are identical in both series (i.e., series A and B). However, our study shows that the AFM IEC was not observed in the undoped series (series A) even in samples having the same structural dimensions as those showing strong AFM IEC in series B. This provides strong evidence that dipole interaction can be eliminated as the primary mechanism for the observed long-range IEC in GaMnAs/GaAs multilayers and points to the importance of carriers in mediating IEC in this system.

One may ascribe long-range IEC to the properties of the Fermi wavelength, which is the fundamental factor for defining the interaction range of the mediating carriers. The Fermi wave vectors is given by $k_F = (3\pi^2 n)^{1/3}$, where n is the carrier concentration. The carrier concentration of ferromagnetic GaMnAs is typically of the order of a few 10^{20} cm^{-3} , which is several orders of magnitude smaller than the carrier concentration in intrinsic metals. This should lead to much longer Fermi wavelengths, $\lambda_F \sim 4 \text{ nm}$, in ferromagnetic semiconductors than in metallic ferromagnets. From this we infer that IEC in magnetic multilayers consisting of ferromagnetic semiconductors such as GaMnAs can have a much longer range. At the same time, our experimental results also suggest that it is important to have a nearly uniform carrier density throughout the superlattice. Thus the effect of band bending near the interface should also be included in theoretical considerations.

IV. CONCLUSIONS

In conclusion, we have reported the observation of the GMR effect in transport properties of GaMnAs-based multilayers. We have confirmed the correlation between the IEC and MR by using two independent experiments: magnetization measurements and polarized neutron reflectometry. The existence of GMR, or lack thereof, is directly related to the type of the IEC present: AFM IEC results in the GMR effect, whereas FM IEC does not. The IEC phase diagram obtained for this material system reflects an oscillatory behavior arising from the dependence of IEC on the GaAs spacer thickness and on carrier concentration in current theory, as expected from current theoretical models. However, our experiment has consistently shown that IEC occurs at much larger structural dimensions than those used in the theoretical calculation. Specifically, the transition between the FM IEC and the AFM IEC is observed for unexpectedly large SL periods ($\sim 34 \text{ ML}$), implying that IEC in this GaMnAs/GaAs system is quite long ranged. A deeper understanding of the carrier-mediated and long-ranged magnetic IEC in GaMnAs/GaAs multilayers is likely to provide new opportunities for magnetic information storage and/or logic devices, in which the spin configurations in the multilayers are controlled via IEC by electrical methods with relatively large structural dimensions.

ACKNOWLEDGMENTS

This research was supported by Basic Science Research Program through the National Research Foundation of Korea (NRF) funded by the Ministry of Education, Science and Technology under Grant No. 2010-0000123; by the Seoul R&BD Program under Grant No. ST090777; and by the National Science Foundation under Grant No. DMR06-03762. J.H.C. was independently supported by the National Research Foundation of Korea through the BAERI program (Grant No. 2010-0017423) and the Basic Research Program (Grant No. 2010-0000594).

*slee3@korea.ac.kr

- ¹M. N. Baibich, J. M. Broto, A. Fert, F. N. Van Dau, F. Petroff, P. Etienne, G. Creuzet, A. Friederich, and J. Chazelas, *Phys. Rev. Lett.* **61**, 2472 (1988).
- ²G. Binasch, P. Grünberg, F. Saurenbach, and W. Zinn, *Phys. Rev. B* **39**, 4828 (1989).
- ³S. A. Wolf, D. D. Awschalom, R. A. Buhrman, J. M. Daughton, S. von Molnar, M. L. Roukes, A. Y. Chtchelkanova, and D. M. Treger, *Science* **294**, 1488 (2001).
- ⁴S. S. P. Parkin, R. F. C. Farrow, R. F. Marks, A. Cebollada, G. R. Harp, and R. J. Savoy, *Phys. Rev. Lett.* **72**, 3718 (1994).
- ⁵P. Grünberg, R. Schreiber, Y. Pang, M. B. Brodsky, and H. Sowers, *Phys. Rev. Lett.* **57**, 2442 (1986).
- ⁶S. S. P. Parkin, N. More, and K. P. Roche, *Phys. Rev. Lett.* **64**, 2304 (1990).
- ⁷S. S. P. Parkin, *Phys. Rev. Lett.* **67**, 3598 (1991).
- ⁸P. J. H. Bloemen, H. W. van Kesteren, H. J. M. Swagten, and W. J. M. de Jonge, *Phys. Rev. B* **50**, 13505 (1994).
- ⁹J. A. Borchers, J. A. Dura, J. Unguris, D. Tulchinsky, M. H. Kelley, C. F. Majkrzak, S. Y. Hsu, R. Loloee, W. P. Pratt, and J. Bass, *Phys. Rev. Lett.* **82**, 2796 (1999).
- ¹⁰H. Kępa, G. Springholz, T. M. Giebultowicz, K. I. Goldman, C. F. Majkrzak, P. Kacman, J. Blinowski, S. Holl, H. Krenn, and G. Bauer, *Phys. Rev. B* **68**, 024419 (2003).
- ¹¹J. J. Rhyne, J. Lin, J. K. Furdyna, and T. M. Giebultowicz, *J. Magn. Magn. Mater.* **177-181**, 1195 (1998).
- ¹²I. Stolichnov, S. W. E. Riestler, H. J. Trodahl, N. Setter, A. W. Rushforth, K. W. Edmonds, R. P. Campion, C. T. Foxon, B. L. Gallagher, and T. Jungwirth, *Nature Mater.* **7**, 464 (2008).
- ¹³H. Ohno, D. Chiba, F. Matsukura, T. Omiya, E. Abe, T. Dietl, Y. Ohno, and K. Ohtani, *Nature (London)* **408**, 944 (2000).
- ¹⁴T. Dietl, H. Ohno, F. Matsukura, J. Cibert, and D. Ferrand, *Science* **287**, 1019 (2000).
- ¹⁵D. Chiba, M. Sawicki, Y. Nishitani, Y. Nakatani, F. Matsukura, and H. Ohno, *Nature (London)* **455**, 515 (2008).
- ¹⁶S. Lee, J. H. Chung, X. Y. Liu, J. K. Furdyna, and B. J. Kirby, *Mater. Today* **12**, 14 (2009).
- ¹⁷F. Maccherozzi, M. Sperl, G. Panaccione, J. Minar, S. Polesya, H. Ebert, U. Wurstbauer, M. Hochstrasser, G. Rossi, G. Woltersdorf, W. Wegscheider, and C. H. Back, *Phys. Rev. Lett.* **101**, 267201 (2008).
- ¹⁸M. Sperl, F. Maccherozzi, F. Borgatti, A. Verna, G. Rossi, M. Soda, D. Schuh, G. Bayreuther, W. Wegscheider, J. C. Cezar, F. Yakhov, N. B. Brookes, C. H. Back, and G. Panaccione, *Phys. Rev. B* **81**, 035211 (2010).
- ¹⁹M. J. Wilson, M. Zhu, R. C. Myers, D. D. Awschalom, P. Schiffer, and N. Samarth, *Phys. Rev. B* **81**, 045319 (2010).
- ²⁰T. Jungwirth, W. A. Atkinson, B. H. Lee, and A. H. MacDonald, *Phys. Rev. B* **59**, 9818 (1999).
- ²¹P. Sankowski and P. Kacman, *Phys. Rev. B* **71**, 201303 (2005).
- ²²A. D. Giddings, T. Jungwirth, and B. L. Gallagher, *Phys. Rev. B* **78**, 165312 (2008).
- ²³K. Szałowski and T. Balcerzak, *Phys. Rev. B* **79**, 214430 (2009).
- ²⁴N. Akiba, F. Matsukura, A. Shen, Y. Ohno, H. Ohno, A. Oiwa, S. Katsumoto, and Y. Iye, *Appl. Phys. Lett.* **73**, 2122 (1998).
- ²⁵D. Chiba, N. Akiba, F. Matsukura, Y. Ohno, and H. Ohno, *Appl. Phys. Lett.* **77**, 1873 (2000).
- ²⁶S. U. Yuldashev, Y. Kim, N. Kim, H. Im, T. W. Kang, S. Lee, Y. Sasak, X. Liu, and J. K. Furdyna, *Jpn. J. Appl. Phys.* **43**, 2093 (2004).
- ²⁷Z. Ge, Y. Y. Zhou, Y. J. Cho, X. Liu, J. K. Furdyna, and M. Dobrowolska, *Appl. Phys. Lett.* **91**, 152109 (2007).
- ²⁸S. J. Chung, S. Lee, I. W. Park, X. Liu, and J. K. Furdyna, *J. Appl. Phys.* **95**, 7402 (2004).
- ²⁹H. Kępa, J. Kutner-Pielaszek, A. Twardowski, C. F. Majkrzak, J. Sadowski, T. Story, and T. M. Giebultowicz, *Phys. Rev. B* **64**, 121302(R) (2001).
- ³⁰J. H. Chung, S. J. Chung, S. Lee, B. J. Kirby, J. A. Borchers, Y. J. Cho, X. Liu, and J. K. Furdyna, *Phys. Rev. Lett.* **101**, 237202 (2008).
- ³¹D. V. Baxter, D. Ruzmetov, J. Scherschligt, Y. Sasaki, X. Liu, J. K. Furdyna, and C. H. Mielke, *Phys. Rev. B* **65**, 212407 (2002).
- ³²K. Y. Wang, K. W. Edmonds, R. P. Campion, L. X. Zhao, C. T. Foxon, and B. L. Gallagher, *Phys. Rev. B* **72**, 085201 (2005).
- ³³H. Kępa, J. Kutner-Pielaszek, J. Blinowski, A. Twardowski, C. F. Majkrzak, T. Story, P. Kacman, R. R. Galazka, K. Ha, H. J. M. Swagten, W. J. M. De Jonge, A. Y. Sipatov, V. Volobuev, and T. M. Giebultowicz, *Europhys. Lett.* **56**, 54 (2001).
- ³⁴Ch. Rehm, D. Nagengast, F. Klose, H. Maletta, and A. Weidinger, *Europhys. Lett.* **38**, 61 (1997).
- ³⁵J. Faure-Vincent, C. Tiusan, C. Bellouard, E. Popova, M. Hehn, F. Moutaigne, and A. Schuhl, *Phys. Rev. Lett.* **89**, 107206 (2002).
- ³⁶Z. Y. Liu and S. Adenwalla, *Phys. Rev. Lett.* **91**, 037207 (2003).
- ³⁷J. A. Borchers, P. M. Gehring, R. W. Erwin, J. F. Ankner, C. F. Majkrzak, T. L. Hylton, K. R. Coffey, M. A. Parker, and J. K. Howard, *Phys. Rev. B* **54**, 9870 (1996).